

## On Steady Weakly Nonlinear Wave Envelopes in Deep Water

M. Magnani<sup>1</sup>, M. Onorato<sup>1</sup>, D. Gunn<sup>2</sup>, M. Rudman<sup>2</sup>, B. Kibler<sup>3</sup>, N. Akhmediev<sup>4</sup>, T. Waseda<sup>5</sup> and A. Chabchoub<sup>6</sup>

<sup>1</sup>Dipartimento di Fisica

Università degli Studi di Torino, 10125 Torino, Italy

<sup>2</sup>Department of Mechanical and Aerospace Engineering  
Monash University, Clayton, Victoria 3800, Australia

<sup>3</sup>Laboratoire Interdisciplinaire Carnot de Bourgogne  
UMR 6303 CNRS-Université de Bourgogne Franche-Comté, 21078 Dijon, France

<sup>4</sup>Research School of Physics and Engineering  
The Australian National University, Canberra, Australian Capital Territory 0200, Australia

<sup>5</sup>Graduate School of Frontier Sciences  
The University of Tokyo, Chiba 277-8561, Japan

<sup>6</sup>Centre for Wind, Waves and Water, School of Civil Engineering  
The University of Sydney, Sydney, New South Wales 2006, Australia

### Abstract

The dynamics of weakly nonlinear wave packets in deep water can be for instance described by the nonlinear Schrödinger equation (NLS). As a deterministic and integrable evolution equation, the NLS enables to determine exact initial or boundary conditions to study the weakly nonlinear motion of a wave packet of interest. Among a vast family of solutions, we will focus our attention on the hydrodynamics of stationary deep water wave packets. The latter can be for instance described by means of hyperbolic or elliptic functions (sech, cnoidal & dnoidal expressions). Experiments have been conducted in different uni-directional wave facilities in order to validate the weakly nonlinear approach. The experimental wave profiles show a very good agreement with NLS predictions for various wave steepness values. The generic effect of wave dissipation in the considered framework will be discussed as well.

**Themes:** Wave Hydrodynamics, Environmental Fluid Mechanics.

### Introduction

Water waves packets are one of most fundamental principles of ocean wave modelling. The accurate description of these is crucial for an improved understanding of water wave physics and ocean engineering application purposes. Indeed, the simplest evolution equation that describes the motion of nonlinear wave packets by taking into account the effect of weak dispersion and non-linearity is the nonlinear Schrödinger equation (NLS). Due to its integrability, the latter framework allows the study of deterministic wave profiles in time and space and most importantly, enables to determine exact initial or boundary conditions to initiate the dynamics of a specific wave profile. Besides the existence of pulsating solutions (breathers), associated to the dynamics of hydrodynamic rogue waves, there is also a hierarchy of stationary packets of cnoidal- and dnoidal-type. These wave envelopes

are of periodic nature while limiting cases of modulation period can either describe a Stokes plane wave or the localized stationary sech-type envelope soliton. In this paper, we report hydrodynamic laboratory observations of such dnoidal and cnoidal wave envelopes over a reasonable propagation distance and different carrier as well as envelope parameters. The experimental and collected data show a very good agreement with NLS predictions for a wide range of steepness values. Moreover, we discuss the effect of dissipation on such periodic and steady wave patterns.

### Weakly nonlinear water wave framework

Given a uni-directional and narrow banded wave field in deep water of wave frequency  $\omega$ , the NLS is known to provide a reasonable approximation for the evolution of the wave envelope  $\Psi$  in time and space [1]

$$i \left( \frac{\partial \Psi}{\partial t} + c_g \frac{\partial \Psi}{\partial x} \right) - \frac{\omega}{8k^2} \frac{\partial^2 \Psi}{\partial x^2} - \frac{\omega k^2}{2} |\Psi|^2 \Psi = 0. \quad (1)$$

The wave number  $k$  can be determined by use of the dispersion relation  $\omega = \sqrt{gk}$  while the group velocity is known to be half the phase speed of the waves, that is  $c_g = \frac{\omega}{2k}$ , while  $g$  denotes the gravitational acceleration. As an integrable dynamical system, it admits a number of relevant deterministic wave envelopes [2, 3]. While breathers are currently widely investigated [4], the relevance of the stationary periodic wave envelopes is not well-studied yet. Indeed, the NLS has two types of steady periodic envelope models: the one-parameter family of the so-called dnoidal waves, parameterised as

$$\Psi_{DN}(x, t) = a \exp \left[ -i(2 - m^2) \frac{a^2 k^2 \omega t}{4} \right] \times \text{dn} \left( \sqrt{2} k^2 a (x - c_g t), m \right), \quad (2)$$

and the cnoidal waves

$$\Psi_{CN}(x,t) = a \exp \left[ -i(2m^2 - 1) \frac{a^2 k^2 \omega t}{4} \right] \quad (3)$$

$$\times m \operatorname{cn} \left( \sqrt{2} k^2 a (x - c_g t), m \right),$$

while the parameter  $0 \leq m \leq 1$ , see [5]. Note that when  $m \rightarrow 1$ , both solutions tend to the well-known sech-type envelope soliton [2, 7].

$$\Psi_{\text{soliton}}(x,t) = a \exp \left( -i \frac{a^2 k^2 \omega t}{4} \right) \quad (4)$$

$$\times \operatorname{sech} \left( \sqrt{2} k^2 a (x - c_g t) \right).$$

On the other hand, when  $m \rightarrow 0$ , both,  $\Psi_{DN}$  and  $\Psi_{CN}$  tend to the constant background of finite amplitude  $a$  and zero, respectively. Note that rogue waves can also arise on dnoidal and cnoidal backgrounds within the fundamental principle of modulation instability, see for instance [8, 9].

### Experimental set-up

The experiments have been conducted in two water wave facilities. While the dnoidal envelopes have been investigated in one of the wave basins of The University of Tokyo with the dimensions  $50 \times 10 \times 5 \text{ m}^3$  [10], the cnoidal wave trains have been studied in a wave flume, installed at Monash University with dimensions  $40 \times 1 \times 1 \text{ m}^3$  [11]. In both facilities, wave gauges have been placed along the flume to measure the free surface elevation. The exact positioning of these will be indicated in the corresponding wave evolution Figures. The boundary conditions applied to the wave maker follows the motion of the surface elevation to first-order of approximation as defined by the NLS at  $x = 0$

$$\eta(t) = \operatorname{Re}(\Psi(t) \exp[i(-\omega t)]). \quad (5)$$

Note that when analysing the collected wave flume measurements, it is important to take into account at least the second-order Stokes correction to the surface elevation due to the nonlinear nature of water waves, that is

$$\eta(t) = \operatorname{Re} \left( \Psi(t) \exp[-i\omega t] + \frac{1}{2} k \Psi^2(t) \exp[-2i\omega t] \right). \quad (6)$$

### Results

We will first illustrate the observations of the dnoidal waves. It is important to choose the carrier parameters, for instance the wave amplitude and wave frequency, in order to satisfy a reasonable steepness value  $\varepsilon = ak$ . This also allows the usage of the NLS approach and the wave maker to generate the waves within the given frequency range. Figure 1 shows the evolution of the dnoidal wave envelopes for carrier amplitude of  $a = 0.02 \text{ m}$ , a steepness of  $\varepsilon = 0.1$  and parameter  $m = 0.5$  as well as the comparison of the in the flume furthest measurement with NLS prediction. The wave train remains indeed stationary, as expected from NLS theory. Interestingly, the modulation instability [12] does not occur even though the wave train is modulated. Another evolution for the same carrier

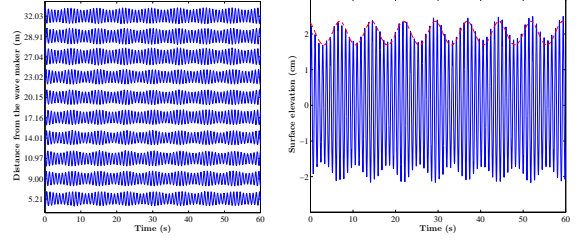


Figure 1: Left: Evolution over 32.03 m of a dnoidal wave envelope for  $a = 0.02 \text{ m}$ ,  $\varepsilon = 0.1$  and  $m = 0.5$ . Right: Comparison of the furthest wave profile measurements, collected 32.03 m from the wave maker (solid blue line) with the NLS wave envelope prediction to second-order in steepness (red dashed line).

parameters, however, for a different parameter  $m = 0.95$  (close to the envelope soliton case) is represented in Figure 2. It is once again clearly noticeable that the wave field remains stationary also in this case.

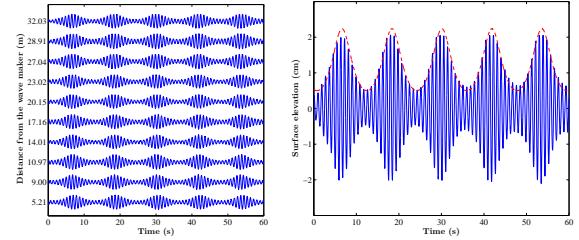


Figure 2: (Left) Evolution over 32.03 m of a dnoidal wave envelope for  $a = 0.02 \text{ m}$ ,  $\varepsilon = 0.1$  and  $m = 0.95$ . (Right) Comparison of the furthest wave profile measurements, collected 32.03 m from the wave maker (solid blue line) with the NLS wave envelope prediction to second-order in steepness (red dashed line).

We can obviously note that the waves become increasingly modulated, when increasing the value of the solution parameter  $m$ . One may suggest that these waves may become unstable following the famed Benjamin-Feir instability [12]. The spectral evolutions reveals the presence of symmetric side-band pairs that are a typical signature of modulated wave trains, see Figure 3. However, in both cases, the modulation frequency as shown in the power spectra in form of side-bands are stable and the modulation instability does not develop [12]. Note that when increasing the value of the parameter  $m$ , we increase the degree of modulation and as such, the number of stable side bands. Moreover, these spectra confirm once again that the corresponding wave trains remain steady. Note that the evolution distance of these experiments are much more significant than in [6] while the agreement with NLS theory is indeed excellent even for a small carrier steepness value of 0.1.

Now, we will turn our attention to the cnoidal wave envelopes. Here, two set of experiments have been conducted to confirm the existence of their dynamics on the water surface. Figure 4 shows the evolution of the stationary cnoidal waves for an amplitude of  $a = 0.02 \text{ m}$ , wave

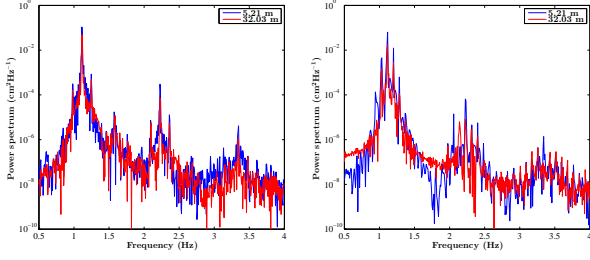


Figure 3: Power spectra of the first wave gauge measurement placed 5.21 m and 32.03 m from the wave maker, respectively. (Left) The wave profiles of Figure 1. (Right) The wave profiles of Figure 2.

steepness  $\varepsilon = 0.12$  and parameter  $m = 0.9$ . Note that the parameter  $m$  is multiplied to the wave amplitude  $a$ , see Equation 3. Thus, the real amplitude of the wave field is effectively 0.018 m. The parameters for the second ex-

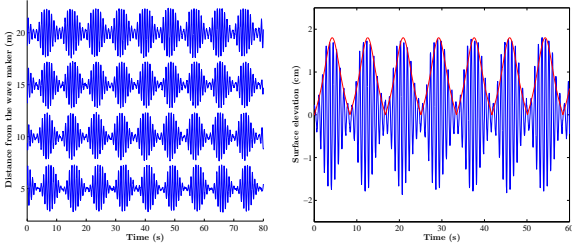


Figure 4: (Left) Evolution over 20 m of a cnoidal wave envelope for  $a = 0.02$  m,  $\varepsilon = 0.12$  and  $m = 0.9$ . (Right) Comparison of the furthest wave profile measurements, collected 20 m from the wave maker (solid blue line) with the NLS wave envelope prediction to second-order in steepness (red dashed line).

periments for cnoidal waves are  $a = 0.04$  m,  $\varepsilon = 0.16$  and  $m = 0.5$ , thus, the effective amplitude is of 0.02 m, see Figure 5. These observations confirm that the from

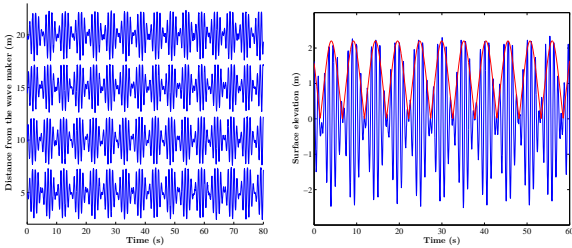


Figure 5: (Left) Evolution over 20 m of a cnoidal wave envelope for  $a = 0.04$  m,  $\varepsilon = 0.16$  and  $m = 0.5$ . (Right) Comparison of the furthest wave profile measurements, collected 20 m from the wave maker (solid blue line) with the NLS wave envelope prediction to second-order in steepness (red dashed line).

the wave maker seeded and generated NLS wave profiles remain stationary when evolving in the flume. The validation with weakly nonlinear theory to second-order of approximation also shows a very good agreement with NLS theory.

One of the most interesting physical features related to these stationary wave envelopes is the fact that these waves are bi-chromatic. Thus, cnoidal envelopes models steady and modulated bi-chromatic water wave groups. This becomes visible, when analysing the power spectra as illustrated in Figure 6. As for the dnoidal waves, the

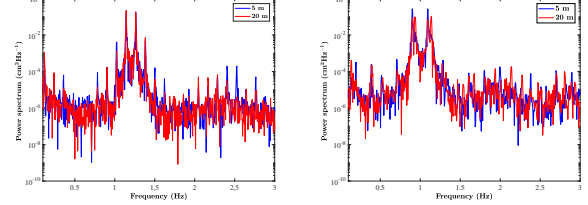


Figure 6: Power spectra of the first wave gauge measurement placed 5 m and 20 m from the wave maker, respectively. (Left) The cnoidal wave profiles of Figure 4. (Right) The cnoidal wave profiles of Figure 5.

spectra do not show any strong deviation during the evolution, confirming steadiness of the waves. Moreover, the double spectral peak is clearly visible as well as the presence of stable side-bands.

### Effect of dissipation

Dissipation is a general limitation, when performing experiments in water wave facilities, particularly, when the wave amplitudes as well as wave lengths considered are small or / and the width of the uni-directional flume is narrow. Recent experiments have shown that these complex effects can be heuristically approximated by extending the NLS by a linear dissipation coefficient as described by [13]

$$i \left( \frac{\partial \Psi}{\partial t} + c_g \frac{\partial \Psi}{\partial x} \right) - \frac{\omega}{8k^2} \frac{\partial^2 \Psi}{\partial x^2} - \frac{\omega k^2}{2} |\Psi|^2 \Psi = -i \mathcal{D} \Psi. \quad (7)$$

In addition, it has been shown that the dissipation is responsible for a typical phase-shift of breathing wave packets and alternates the dynamics between the envelope crests and troughs [13]. In order to investigate the linear dissipative effects on dnoidal and cnoidal wave envelopes, we performed numerical NLS simulations using the split step method. The first case shows the result for a dnoidal wave packet with parameters  $m = 0.95$ ,  $\varepsilon = 0.1$  and  $a = 0.02$  m, as shown in Figure 2 while the amplitude dissipation rate has been chosen to be of 30% over 100 m of propagation. Similar simulations have been performed for a cnoidal wave profile with parameters  $m = 0.5$ ,  $\varepsilon = 0.16$  and  $a = 0.04$  m for the same dissipation rate of 30%, the case shown in Figure 5. The simulations results are illustrated in Figure 7. Clearly, the effect of linear dissipation on dnoidal waves is responsible for the attenuation of the envelope to a quasi-constant background followed by a phase-shift as in the case for Akhmediev breathers [13]. The characteristic and typical envelope attenuation process has been already observed in [6], however, it has been attributed to the frequency- and amplitude-dispersion imbalance. In contrast, dissi-

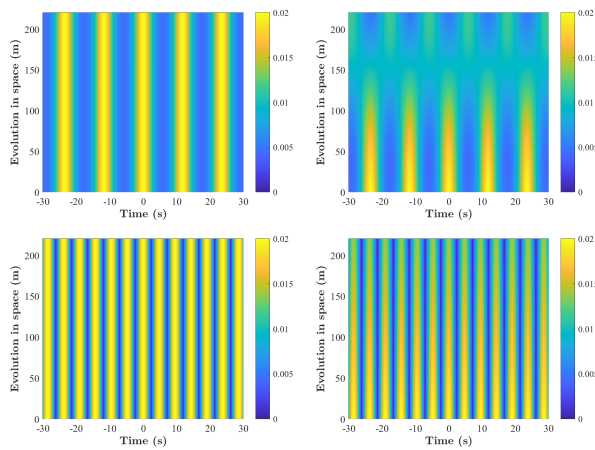


Figure 7: Dimensional numerical NLS simulations of a dnoidal and cnoidal wave envelope evolution. Top: dnoidal waves for  $m = 0.95$  and carrier parameter  $\epsilon = 0.1$  and  $a = 0.02$  m. Top left: Conservative evolution. Top right: Dissipative evolution with an amplitude attenuation of 30% over 100 m of wave propagation. Bottom: cnoidal waves for  $m = 0.5$  and carrier parameter  $\epsilon = 0.16$  and  $a = 0.04$  m. Bottom left: Conservative evolution. Bottom right: Dissipative evolution with an amplitude attenuation of 30% over 100 m of wave propagation.

pative cnoidal envelopes just attenuate in amplitude and do not imply any phase-shift dynamics. The effect of linear dissipation is an interesting feature that needs further attention and motivates further experiments in larger hydrodynamic facilities.

## Conclusion

We have experimentally investigated the hydrodynamics of periodic stationary wave envelopes in deep water. The results confirm the steadiness and wave envelope symmetry of dnoidal and cnoidal envelope solutions of the NLS over a large propagation distance, when setting the wave maker's motion with the corresponding exact deterministic wave profiles, accordingly. Furthermore, we have also discussed the effect of linear dissipation on these periodic patterns. Future work will be devoted to investigate and detect such phase-shift effects in laboratory environments. Moreover, restricting the range of parameters and characterising the limitations of the approach, by conducting experiments in larger water wave facilities and performing fully nonlinear simulations [14, 15] will be subject of further studies as well.

## References

[1] Zakharov, V. E., Stability of periodic waves of finite amplitude on the surface of a deep fluid, *Journal of Applied Mechanics and Technical Physics*, **9**, 1968, 190–194.

[2] Shabat, A. and Zakharov, V. E., Exact theory of two-dimensional self-focusing and one-dimensional self-modulation of waves in nonlinear media, *Soviet physics JETP*, **34**, 1972, 62–69.

[3] Akhmediev, N. and Ankiewicz, A., *Solitons: nonlinear pulses and beams*, Chapman & Hall, 1997.

[4] Chabchoub, A., Onorato, M. and Akhmediev, N., *Hydrodynamic Envelope Solitons and Breathers, Rogue and Shock Waves in Nonlinear Dispersive Media*, Springer, 2016, 55–87.

[5] Dysthe, K. B. and Trulsen, K., Note on breather type solutions of the NLS as models for freak-waves, *Physica Scripta*, **T82**, 1999, 48–52.

[6] Pierson, W. Jr., Donelan, M. A. and Hui, W. H., Linear and nonlinear propagation of water wave groups, *Journal of Geophysical Research: Oceans*, **97**, 1992, 5607–5621.

[7] Yuen, H. C. and Lake, B. M., Nonlinear deep water waves: Theory and experiment, *Physics of Fluids*, **18**, 1975, 956–960.

[8] Kedziora, D. J., Ankiewicz, A. and Akhmediev, N., Rogue waves and solitons on a cnoidal background, *The European Physical Journal - Special Topics*, **223**, 2014, 43–62.

[9] Chen, J. and Pelinovsky, D. E., Rogue periodic waves of the focusing nonlinear Schrödinger equation, *Proceedings of the Royal Society A*, **474**, 2018, 20170814.

[10] Mozumi, K., Waseda, T. and Chabchoub, A., 3D stereo imaging of abnormal waves in a wave basin, *ASME 2015 34th International Conference on Ocean, Offshore and Arctic Engineering. American Society of Mechanical Engineers*, 2015.

[11] Gunn, D. F., Rudman, M., Cohen, R. C. Z. and Chabchoub, A. Modelling First and Second Order Rogue Waves using 2D SPH, *The Twenty-fifth International Ocean and Polar Engineering Conference. International Society of Offshore and Polar Engineers*, 2015.

[12] Benjamin, T. B. and Feir, J. E., The disintegration of wave trains on deep water Part 1. Theory, *Journal of Fluid Mechanics*, **27**, 1967, 417–430.

[13] Kimmoun, O., Hsu, H. C., Branger, H., Li, M. S., Chen, Y. Y., Kharif, C., Onorato, M., Kelleher, E. J. R., Kibler, B., Akhmediev, N. and Chabchoub, A., Modulation instability and phase-shifted Fermi-Pasta-Ulam recurrence, *Scientific Reports*, **6**, 2016, 28516.

[14] Slunyaev, A. V., and Shrira, V. I., On the highest non-breaking wave in a group: fully nonlinear water wave breathers versus weakly nonlinear theory, *Journal of Fluid Mechanics*, **735**, 2013, 203–248.

[15] Chabchoub, A., Waseda, T., Kibler, B. and Akhmediev, N., Experiments on higher-order and degenerate Akhmediev breather-type rogue water waves, *Journal of Ocean Engineering and Marine Energy*, **3**, 2017, 385–394.